Electronic Supplementary Material (ESI) for Journal of Materials Chemistry C.

Realizing of a broad-scope and high-sensitivity optical thermometer based on dual-emission centers with structure confinement effect-related energy transfer

Shixiang Huang[a, #], Liuhan Yi[a, #], Feng Zhang[a,*], Xiansheng Liu[a], Chao Li[a,*], Mengzhu Long[a], and Yuhua Wang[b]

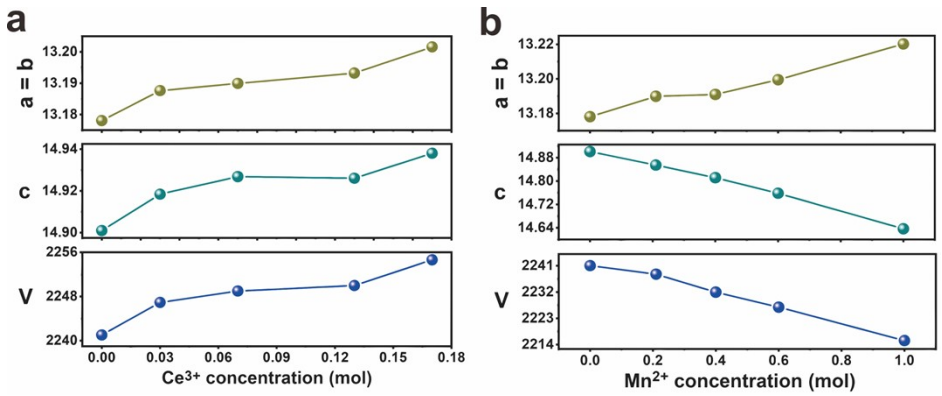

Figure S1 (a) and (b) respectively give the lattice parameters and the unit cell volume depending on the Ce^{3+} and Mn^{2+} contents in $K_7CaLu_2B_{15}O_{30}$.

Table S1 The radius percentage difference between matrix cations and doped ions.

Matrix cation	Coordination number (n)	Radius (Å)	Dr (%)	
			Ce^{3+} (n = 6, r = 1.01 Å; n = 8, r = 1.14 Å)	Mn^{2+} (n = 6, r = 0.67 Å; n = 8, r = 0.96 Å)
$K^+(1)$	8	1.51	24.30	36.40
$K^+(2)$	6	1.38	26.80	51.40
$K^+(3)$	6	1.38	26.80	51.40
Ca^{2+}	6	1.00	**-1.00**	**33.00**
Lu^{3+}	6	0.86	**-17.30**	**22.20**
Y^{3+}	6	0.90	**-12.20**	**26.60**
Gd^{3+}	6	0.94	**-7.7**	**28.60**

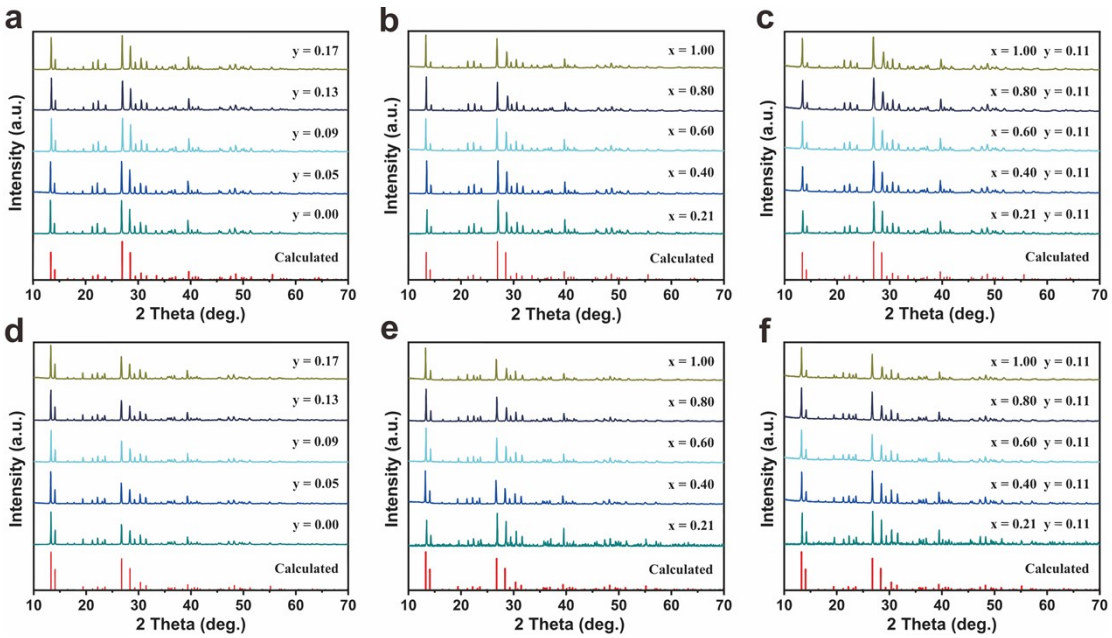

Figure S2 (a) and (b) respectively show the XRD patterns of $K_7CaY_2B_{15}O_{30}:Ce^{3+}$ with different Ce^{3+} concentrations and $K_7CaY_2B_{15}O_{30}:Mn^{2+}$ with varied Mn^{2+} contents. (c) gives the XRD patterns of the $K_7CaY_2B_{15}O_{30}$:11%Ce^{3+}, xMn^{2+} samples ($0 \le x \le 1$). (d) - (f) display the XRD patterns of the samples $K_7CaGd_2B_{15}O_{30}:yCe^{3+}$ ($0 \le y \le 0.17$), $K_7CaGd_2B_{15}O_{30}:xMn^{2+}$ ($0 \le x \le 1$), and $K_7CaGd_2B_{15}O_{30}$:11%Ce^{3+}, xMn^{2+} ($0 \le x \le 1$).

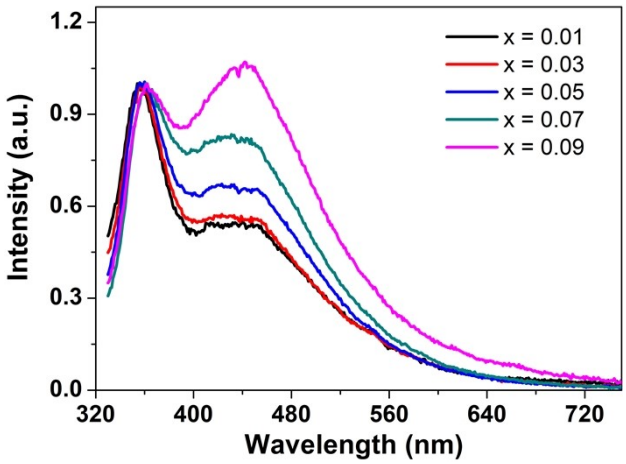

Figure S3 Height-normalized emission spectra around 360 nm (λ_{ex} = 310 nm) of $K_7CaLu_2B_{15}O_{30}$:xCe^{3+} (x = 0.01, 0.03, 0.05, 0.07, 0.09) samples at room temperature.

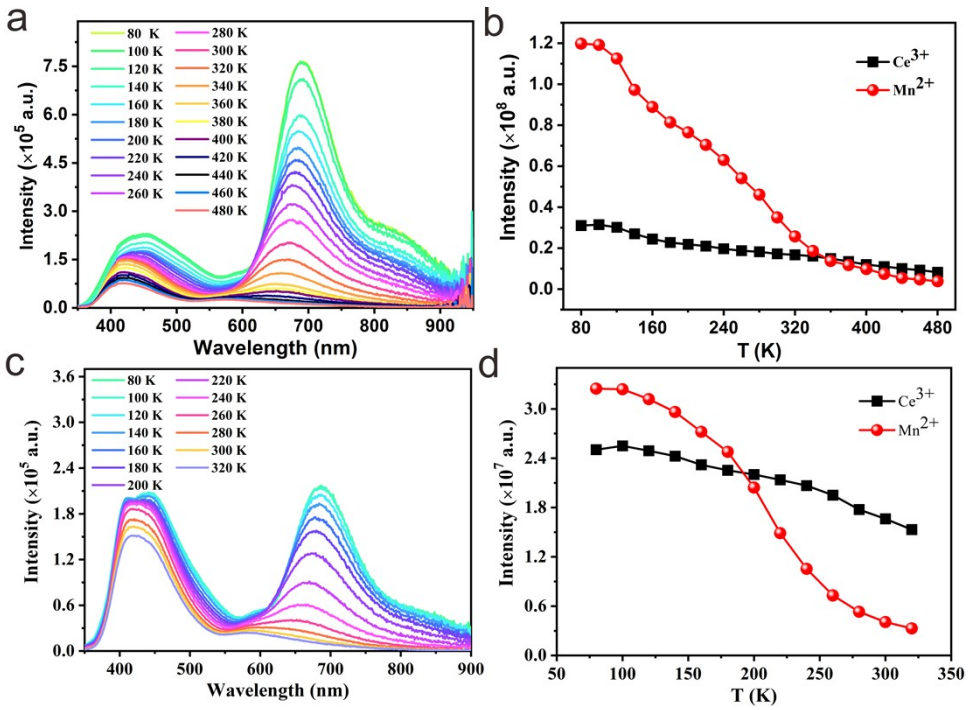

Figure S4 (a) The emission spectra of $K_7CaY_2B_{15}O_{30}$:0.11Ce^{3+}, 0.25Mn^{2+} (λ_{ex} = 329 nm) depending on the temperature (80 - 480 K). (b) The temperature dependent emission intensity of Ce^{3+} and Mn^{2+} in $K_7CaY_2B_{15}O_{30}$. (c) The emission spectra of $K_7CaGd_2B_{15}O_{30}$:0.11Ce^{3+}, 0.25Mn^{2+} (λ_{ex} = 327 nm) depending on the temperature (80 - 320 K). (d) The temperature dependent emission intensity of Ce^{3+} and Mn^{2+} in $K_7CaGd_2B_{15}O_{30}$.

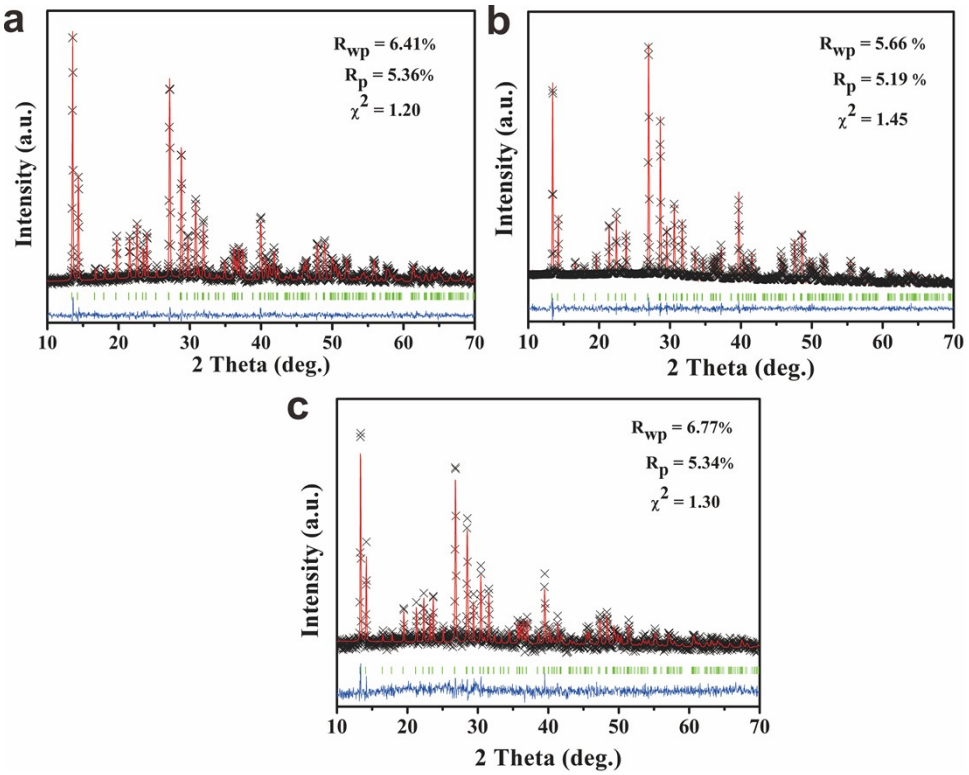

Figure S5 (a)-(c) Rietveld refinement of the XRD profile of $K_7CaLn_2B_{15}O_{30}$:0.11Ce^{3+}, 0.25Mn^{2+} (Ln = Lu,Y, Gd).

Table S2. Crystallographic data, refinement parameters, and selected bond lengths for $K_7CaLn_2B_{15}O_{30}$:0.11Ce^{3+}, 0.25Mn^{2+} (Ln = Lu, Y, Gd)

	KCLBO:0.11Ce^{3+}, 0.25Mn^{2+}	KCYBO:0.11Ce^{3+}, 0.25Mn^{2+}	KCGBO:0.11Ce^{3+}, 0.25Mn^{2+}
cryst. syst.	trigonal	trigonal	trigonal
space group	*R*32	*R*32	*R*32
a (Å)	13.2032(0)	13.2835(6)	13.3562(4)
c (Å)	14.8639(6)	14.9441(0)	14.9963(9)
V (Å^3)	2243.993	2283.652	2316.784
R_{wp} (%)	6.41	5.66	6.77
R_p(%)	5.36	5.19	5.34
χ^2	1.20	1.45	1.30
Ln-O (Å)	Lu(1)-O(1) 2.384(26)×3 Lu(1)-O(1) 2.438(26)×3	Y(1)-O(1) 2.269(25)×3 Y(1)-O(1) 2.377(30)×3	Gd(1)-O(1) 2.215(50)×3 Gd(1)-O(1) 2.748(20)×3
Ca-O (Å)	Ca(1)-O(4) 2.3950(9) Ca(1)-O(4) 2.3940(9) Ca(1)-O(4) 2.3949(9) Ca(1)-O(4) 2.3941(9) Ca(1)-O(4) 2.3936(9) Ca(1)-O(4) 2.3938(9)	Ca(1)-O(4) 2.4036(5) Ca(1)-O(4) 2.4035(5) Ca(1)-O(4) 2.4027(5) Ca(1)-O(4) 2.4023(5) Ca(1)-O(4) 2.4031(5) Ca(1)-O(4) 2.4023(5)	Ca(1)-O(4) 2.3476(11) Ca(1)-O(4) 2.3466(11) Ca(1)-O(4) 2.3468(11) Ca(1)-O(4) 2.3470(11) Ca(1)-O(4) 2.3478(11) Ca(1)-O(4) 2.3480(11)

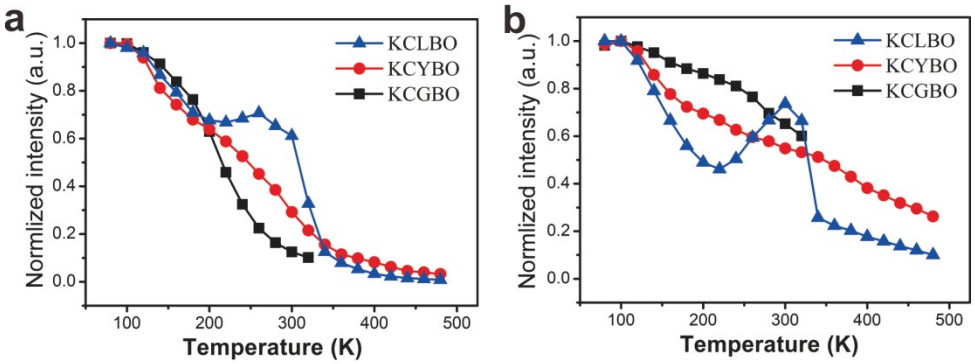

Figure S6 (a) The normalized integral intensity of Mn^{2+} depend on the temperature in $K_7CaLn_2B_{15}O_{30}$:0.11Ce^{3+}, 0.25Mn^{2+} (Ln = Y, La, Gd). (b) The normalized integral intensity of Ce^{3+} depend on the temperature in $K_7CaLn_2B_{15}O_{30}$:0.11Ce^{3+}, 0.25Mn^{2+} (Ln = Y, La, Gd).